J Mol Model (2013) 19:3263–3270
DOI 10.1007/s00894-013-1865-1

ORIGINAL PAPER

# Theoretical investigation of the gas-phase reactions of $CF_2ClC(O)OCH_3$ with the hydroxyl radical and the chlorine atom at 298 K

**Bhupesh Kumar Mishra · Arup Kumar Chakrabartty · Ramesh Chandra Deka**

Received: 5 February 2013 / Accepted: 19 April 2013 / Published online: 8 May 2013


**Abstract** A Theoretical study on the mechanism of the reactions of $CF_2ClC(O)OCH_3$ with the OH radical and Cl atom is presented. Geometry optimization and frequency calculations have been performed at the MPWB1K/6-31+G(d,p) level of theory and energetic information is further refined by calculating the energy of the species using G2(MP2) theory. Transition states are searched on the potential energy surface involved during the reaction channels and each of the transition states are characterized by presence of only one imaginary frequency. The existence of transition states on the corresponding potential energy surface is ascertained by performing intrinsic reaction coordinate (IRC) calculation. Theoretically calculated rate constants at 298 K and atmospheric pressure using the canonical transition state theory (CTST) are found to be in good agreement with the experimentally measured ones. Using group-balanced isodesmic reactions as working chemical reactions, the standard enthalpies of formation for $CF_2ClC(O)OCH_3$, $CF_2ClC(O)OCH_2$ and $CF_3C(O)OCH_3$ are also reported for the first time.

**Keywords** Bond dissociation energy · Chloro-fluoroesters · Isodesmic reactions · Rate constant

**Electronic supplementary material** The online version of this article (doi:10.1007/s00894-013-1865-1) contains supplementary material, which is available to authorized users.

B. K. Mishra · A. K. Chakrabartty · R. C. Deka (✉)
Department of Chemical Sciences, Tezpur University, Napaam, Tezpur, Assam 784 028, India
e-mail: ramesh@tezu.ernet.in

## Introduction

It is now a well recognized fact that atomic chlorine transported to the stratosphere on account of release of a variety of chlorine containing compounds particularly chlorofluorocarbons (CFCs) into the atmosphere are responsible for the catalytic destruction of ozone in the atmosphere [1, 2]. Recently, hydrofluoroethers (HFEs) and some hydrochlorofluoroethers (HCFEs) have been the focus of intense attention as replacement materials for CFCs and hydrochlorofluorocarbons (HCFCs) in applications such as heat-transfer fluid in refrigeration systems, cleaning agent in electronic industry, foam-blowing, lubricant deposition and also as anesthetics [3–6]. The absence of chlorine atoms in HFEs shows that such compounds would have little impact on stratospheric ozone and that they would possess a negligible ozone depleting potential (ODP), whereas the presence of chlorine atom in HCFEs would confer them greater ozone-depleting potentials (ODP) compared to HFEs [7, 8]. The understanding of the degradation mechanism of both HFEs and HCFEs are an important area of recent research to determine the impact of these compounds on atmospheric pollution and global warming. Therefore, considerable attention has been paid in recent years to perform experimental and theoretical studies on the decomposition kinetics of these partially halogenated ethers [8–16]. It is a well known fact that fluorinated esters (FESs) are the primary products of the atmospheric oxidation of HFEs [17]. Like most volatile organic compounds, FESs containing C–H bonds are removed from the troposphere by reactions with atmospheric oxidants, OH radicals being the most dominant oxidant [18]. Although the reaction with OH radicals constitutes the

main tropospheric sink of HFEs, the chlorine atom plays an important role in atmospheric chemistry [19]. In fact, chlorine atoms have been monitored in concentrations on the order of $10^4$ molecule $cm^{-3}$ over the marine boundary layer [20]. Like FESs chlorinated fluoroesters (CFESs) may arise from both anthropogenic and natural sources and produced in the atmosphere by photochemical degradation and atmospheric oxidation of hydrochlorofluoroethers (HCFEs) [21]. Quan et al. [22] have synthesized chlorofluoroacetates by defluorination of chlorofluoroethers using porous aluminum fluoride (PAF). Sekiya and co-workers [23] reported that defluorination reaction of 2-chloro-1,1,2,2-tetrafluoro ethyl methyl ether to methyl chlorodifluoroacetate ($CF_2ClC(O)OCH_3$) proceeded in 67 % using PAF. Nevertheless, CFESs like $CF_2ClC(O)OCH_3$ are also expected to emit directly into the atmosphere due to their extensive use in laboratory as a building blocks of various valuable organic intermediates [24–26]. These CFESs are removed from the troposphere mainly by reaction with OH radicals [27]. In order to evaluate the possible contribution of the photooxidation of CFESs in the environment, knowledge of the rate coefficients for reactions of CFESs with tropospheric oxidants such as OH radicals and Cl atoms as well as associated degradation pathways and product distributions are vital. In this work, kinetic and mechanistic studies have been performed at atmospheric pressure and room temperature for the reactions of OH radical and Cl atom with methyl chlorodifluoroacetate ($CF_2ClC(O)OCH_3$). To the best of our knowledge, the reactions of $CF_2ClC(O)OCH_3$ with OH radical and Cl atom have been experimentally investigated by Blanco and Teruel [28]. They studied the hydrogen abstraction reactions of hydroxyl radicals and chlorine atoms with methyl chlorodifluoroacetate ($CF_2ClC(O)OCH_3$) and ethyl chlorodifluoroacetate ($CF_2ClC(O)OCH_2CH_3$) by the relative kinetic method at 298 K and atmospheric pressure (760 Torr). The experimental rate constants were derived as $k_1(OH + CF_2ClC(O)OCH_3) = (1.1 \pm 0.3) \times 10^{-13}$ cm$^3$ molecule$^{-1}$ s$^{-1}$ and $k_2(Cl + CF_2ClC(O)OCH_3) = (1.0 \pm 0.2) \times 10^{-13}$ cm$^3$ molecule$^{-1}$ s$^{-1}$ [28]. In other reports, Blanco et al. [29, 30] studied the kinetics of the reactions of OH radical and Cl atom with selected fluoroacetates by the relative kinetic method at 298±2 K and atmospheric pressure (760±10 Torr). However, experimental studies provided only the total rate constant and it is difficult to predict the detailed mechanism, thermo chemistry and contribution of each reaction channel toward overall rate constant. Therefore in our present study, we have performed a detailed theoretical study for the first time on the above mentioned H-abstraction reactions of methyl chlorodifluoroacetate ($CF_2ClC(O)OCH_3$).

Our calculation indicates that two reaction channels are feasible for the $CF_2ClC(O)OCH_3$ + OH/Cl as given below.

$$CF_2ClC(O)OCH_3 + OH \rightarrow CF_2ClC(O)OCH_2 + H_2O \quad (R1)$$

$$CF_2ClC(O)OCH_3 + Cl \rightarrow CF_2ClC(O)OCH_2 + HCl \quad (R2)$$

There may be also the possibility of OH/Cl addition to the carbonyl (>C=O) carbon atom of $CF_2ClC(O)OCH_3$. However, recent experimental and theoretical study on esters and halogenated esters suggest that H-abstraction is the dominant pathway for degradation under atmospheric conditions. Accordingly, in our present study we pay our attention mainly toward the H-abstraction rather than addition reactions of $CF_2ClC(O)OCH_3$ by OH radical and Cl atom [17, 31, 32]. In addition, the knowledge of accurate enthalpy of formation ($\Delta_fH°_{298}$) for $CF_2ClC(O)OCH_3$ and $CF_2ClC(O)OCH_2$ is of vital importance for determining the thermodynamic properties and the kinetics of atmospheric process. However, no theoretical or experimental study of standard enthalpy has been reported for these two species. Here, we predict the enthalpies of formation using isodesmic reactions by performing single-point energy calculation at high level of theory, namely, G2(MP2) with geometry parameters obtained at the MPWB1K/6-31+G(d,p) level.

## Computational methods

Ab-initio quantum mechanical calculations were performed with the Gaussian 09 suite of program [33]. Geometry optimization of the reactant, products and transition states were made at the MPWB1K level of theory [34] using 6-31+G(d,p) basis set. The hybrid meta-density functional, MPWB1K has been found to give excellent results for thermochemistry and kinetics and is known to produce reliable results [35, 36]. In order to determine the nature of different stationary points on the potential energy surface, vibrational frequencies calculations were performed using the same level of theory at which the optimization was made. All the stationary points had been identified to correspond to stable minima by ascertaining that all the vibrational frequencies had real positive values. The transition states were characterized by the presence of only one imaginary frequency (NIMAG=1). To ascertain that the identified transition states connect reactant and products smoothly, intrinsic reaction coordinate (IRC) calculations [37] were performed at the MPWB1K/6-31+G(d,p) level. To obtain more accurate energies and barrier heights, the energies are refined by using a potentially high-level method such as G2(MP2) [38]. In this method, the geometry and frequency calculations were performed at MPWB1K/6-31+G(d,p) level. The ZPE thus, obtained was corrected with a scale factor of 0.9537 to partly eliminate the systematic errors [34].

## Results and discussion

The detailed thermodynamic calculations performed at MPWB1K/6-31+G(d,p) and G2(MP2) levels for reaction enthalpies and free energies associated with reaction channels (1–2) are listed in Table 1. The enthalpy of reaction ($\Delta_r H^0_{298}$) values tabulated in Table 1 for R1 and R2 show that both the reactions are exothermic in nature and thermodynamic facile. The $\Delta_r H^0_{298}$ values obtained from the G2(MP2) and MPWB1K methods for R1 at 298 K differ by 2.68 kcal mol$^{-1}$ whereas the same for R2 differ by only 1.18 kcal mol$^{-1}$. The small difference suggests that the MPWB1K method provides thermochemical data which are comparable to the much more expensive G2(MP2) method. The optimized geometries of reactants, products and transition states along with structural parameters obtained at MPWB1K/6-31+G(d,p) level are shown in Fig. 1. It can be seen that the calculated bond distances for OH, HCl and $H_2O$ at MPWB1K level show good mutual agreement with the corresponding experimental values [39]. Transition states searched on the potential energy surfaces of reactions (1–2) and are characterized as $TS_{OH}$ and $TS_{Cl}$, respectively. The search was made along the minimum energy path on a relaxed potential energy surface. The TS structure for H abstraction by OH radical as shown in Fig. 1 followed by visualization of the optimized geometry using ChemCraft [40] reveals that the breaking bond C–H (C3–H3) increases from 1.080 to 1.286 Å (19 % increase) whereas the newly formed H–O bond (H3–O3) is increased from 0.960 to 1.261 Å resulting in an increase of about 31 %. The fact that the elongation of the breaking bond is shorter than that of the forming bond indicates that the barrier of the reaction is near the corresponding reactants. This means the reaction will proceed via early transition state structure which is in consonance with Hammond's postulate [41] applied to an exothermic hydrogen abstraction reaction. While for the transition state, $TS_{Cl}$ of the $CF_2ClC(O)OCH_3$+Cl reaction, the elongation of the breaking C–H bond (C3–H3) is found to be 1.080 to 1.390 Å resulting in an increase of about 28 %. The forming H–Cl bond is elongated from 1.275 to 1.452 Å (13 %) with respect to the equilibrium bond length in an isolated molecule HCl. The elongation of the breaking bond is greater than that of the forming bond indicating that the TS is product like, i.e., the reaction will proceed via late TS. This can be put in a more quantitative manner, if one calculates the quantity $R_b$ [42]. The $R_b$ value should be less than 0.5 for early TS. The $R_b$ values calculated from the MPWBIK/6-31+G(d,p) optimized structures are 0.45 and 0.67 for the $TS_{OH}$ and $TS_{Cl}$, respectively. These values indicate that the $TS_{OH}$ is more like the reactant than the products (early) while $TS_{Cl}$ is more like the product than the reactants, i.e., late TS.

**Table 1** Thermochemical data for the H abstraction reaction channels of $CF_2ClC(O)OCH_3$ calculated at MPWB1K/6-31+G(d,p) and G2(MP2) (within parenthesis) level of theories. All values are in kcal mol$^{-1}$

| Reaction channels | $\Delta_r H°_{298}$ | $\Delta_r G°_{298}$ |
|---|---|---|
| Reaction 1 | −14.84 (−17.52) | −16.17 (−19.80) |
| Reaction 2 | −0.69 (−1.87) | −3.26 (−5.28) |

Table 2 presents the harmonic vibrational frequencies of all the stationary points involved in reactions (1–2) as well as the reliable experimental values. All the reactants and products were identified with zero imaginary frequency (NIMAG=0), and transition states, $TS_{OH}$ and $TS_{Cl}$ were identified with one imaginary frequency at 1548 and 1006 cm$^{-1}$ corresponding to the reaction coordinate. Intrinsic reaction path calculations (IRC) have also been performed for each transition states at the same level of theory using the Gonzalez-Schlegel steepest descent path in the mass-weighted Cartesian coordinates with a step size of 0.01(amu$^{1/2}$-bohr). The IRC plots for $TS_{OH}$ and $TS_{Cl}$ shown in Figs. S1 and S2 in Supporting information reveal that the transition state structures connect smoothly the reactant and the product sides. The energies of reactants, transition states and products obtained in the IRC calculations are given in Table S1 in Supporting information and they are in excellent agreement with the individually optimized values at MPWB1K/6-31+G(d,p) level of theory.

Zero-point corrected total energies for various species and transition states involved in the reactions (1–2) calculated at MPWB1K and G2(MP2) are tabulated in Table 3. The associated energy barrier corresponding to reactions (1–2) are also recorded in Table 3. The G2(MP2) calculated barrier heights for R1 ($TS_{OH}$) and R2 ($TS_{Cl}$) are 2.59 and 1.42 kcal mol$^{-1}$, respectively, whereas these values are 2.24 and 2.04 kcal mol$^{-1}$ at the MPWB1K level. The barrier heights obtained from the G2(MP2) results are only 0.35 to 0.62 kcal mol$^{-1}$ higher than that obtained at the MPWB1K level. An extensive literature survey reveals the absence of any experimental or theoretical data available for making a comparison of these values. However, an intensive ab-initio calculation performed in our previous study [35] for a similar species, $CF_3C(O)OCH_3$ (MTFA) yielded a value of 2.95 and 1.76 kcal mol$^{-1}$, respectively for hydrogen abstraction by OH and Cl atom at G2(MP2)//MPWB1K/6-31+G(d,p) level. The lowering of barrier heights in case of $CF_2ClC(O)OCH_3$ is expected due to replacement of more electronegative F atom in $CF_3C(O)OCH_3$ by Cl atom in $CF_2ClC(O)OCH_3$. A schematic potential energy surface of the $CF_2ClC(O)OCH_3$+OH/Cl reactions obtained at the G2(MP2)//MPWB1K/6-31+G(d,p)+ZPE level is plotted and shown in Fig. 2. In the construction of energy diagram, zero-point corrected total energies as recorded in Table 3 are utilized. These energies are plotted with respect to the

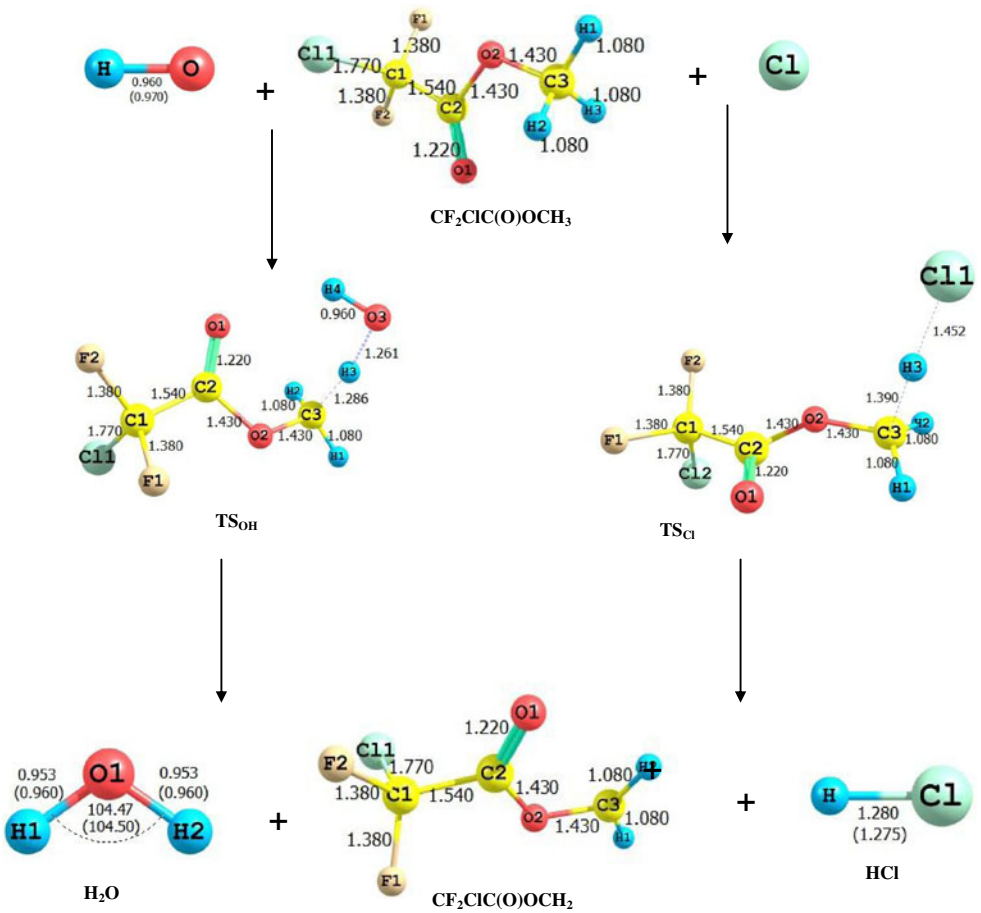


**Fig. 1** Optimized geometries of reactants, products and transition state involved in the H-atom abstraction reaction of $CF_2ClC(O)OCH_3$ by OH radical and Cl atom using MPWB1K/6-31+G(d,p) method. The experimental values are given in *parentheses*

ground state energy of $CF_2ClC(O)OCH_3$+OH/Cl arbitrarily taken as zero. The values in parentheses shown in Fig. 2 are ZPE corrected values obtained at MPWB1K/6-31+G(d,p) level. The barrier height for H abstraction by Cl atom is about 1.17 kcal $mol^{-1}$ lower than that for H abstraction by OH radical at G2(MP2) level. Spin contamination is not important for the $CF_2ClC(O)OCH_3$ because $<S^2>$ is found to be 0.76 at MPWB1K/6-31+G(d,p) before annihilation that is only slightly larger than the expected value of $<S^2> = 0.75$ for doublets.

Table 4 lists the calculated bond-dissociation energies, BDE ($D^0_{298}$) of the C–H bonds of $CF_2ClC(O)OCH_3$ and $CF_3C(O)OCH_3$ molecules along with some experimental data. Our G2(MP2) calculated $D^0_{298}$ value for the C–H bond in $CF_2ClC(O)OCH_3$ is 102.13 kcal $mol^{-1}$ which is about 8.19 kcal $mol^{-1}$ lower than the $D^0_{298}$ value for the C–H bond

**Table 2** Unscaled vibrational frequencies of reactants, products and transition states at MPWB1K/6-31+G(d,p) level of theory

| Species | Vibrational frequencies ($cm^{-1}$) |
|---|---|
| $CF_2ClC(O)OCH_3$ | 43, 116, 168, 190, 243, 326, 353, 378, 448, 533, 650, 769, 860, 1014, 1083, 1211, 1215, 1263, 1287, 1429, 1523, 1527, 1529, 1945, 3150, 3243, 3282 |
| $TS_{OH}$ | 1548i, 30, 51, 103, 141, 189, 254, 322, 332, 351, 377, 384, 449, 534, 651, 693, 769, 853, 915, 1019, 1118, 1136, 1218, 1267, 1293, 1341, 1431, 1480, 1508, 1936, 3189, 3306, 3876 |
| $TS_{Cl}$ | 1006i, 21, 34, 55, 131, 197, 245, 334, 370, 411, 449, 506, 537, 651, 759, 840, 973, 1007, 1027, 1152, 1232, 1237, 1283, 1300, 1396, 1499, 1966, 3205, 3342 |
| $CF_2ClC(O)OCH_2$ | 43, 122, 192, 218, 239, 295, 335, 372, 381, 448, 534, 650, 752, 840, 1012, 1155, 1212, 1266, 1301, 1406, 1490, 1943, 3288, 3452 |
| OH | 3868 |
| $H_2O$ | 1637, 3975, 4101 |
| HCl | 3084 |

**Table 3** Zero-point corrected total energy for the reactants, products and transition states along with the associated energy barrier, ΔE (kcal mol$^{-1}$). All other values are in hartree

| Species | MPWB1K | ΔE | G2(MP2) | ΔE |
|---|---|---|---|---|
| $CF_2ClC(O)OCH_3$+OH | −1001.966757 | 0.00 | −1001.105964 | 0.00 |
| $CF_2ClC(O)OCH_3$+Cl | −1386. 454666 | 0.00 | −1385.151997 | 0.00 |
| $TS_{OH}$ | −1001.963183 | 2.24 | −1001.101827 | 2.59 |
| $TS_{Cl}$ | −1386.451348 | 2.08 | −1385.149726 | 1.42 |
| $CF_2ClC(O)OCH_2$+$H_2O$ | −1001.991069 | −15.25 | −1001.134556 | −17.94 |
| $CF_2ClC(O)OCH_2$+HCl | −1386.456614 | −1.22 | −1385.156545 | −2.85 |

in $CF_3C(O)OCH_3$ (110.32 kcal mol$^{-1}$). The high $D^0_{298}$ of the C–H bond in $CF_3C(O)OCH_3$ is due to the combined electron-withdrawing inductive effects of three F atoms. At the same level, the $D^0_{298}$ (C–O) values for $CF_2ClC(O)OCH_3$ obtained through two pathways are 103.20 and 95.83 kcal mol$^{-1}$, respectively. No comparison between theory and experiment can be made due to the lack of the experimental $D^0_{298}$ (C–O) values. In order to check accuracy of the calculations, the value of BDE of the O–H bond in the water molecule has been computed and compared to the literature data. The experimental value of $D^0_{298}$ of the O–H bond in water is 119.0 kcal mol$^{-1}$ [43]. $D^0_{298}$ calculated at the G2(MP2)//MPWB1K/6-31+G(d,p) level, in this work, is 119.2 kcal mol$^{-1}$. Thus, the value of $D^0_{298}$ of the O–H bond in water, obtained at the theoretical level applied in this work, almost reproduces the experimental value. Moreover, our G2(MP2) calculated $D^0_{298}$ value for the H–Cl bond (104.0 kcal mol$^{-1}$) is also in excellent agreement with the experimental value of 103.1 kcal mol$^{-1}$ [43]. The good agreement between the theoretical and experimental above-mentioned results implies that the G2(MP2)//MPWB1K/6-31+G(d,p) level is a suitable method to compute the bond dissociation energies and our calculated $D^0_{298}$ (C–H) and $D^0_{298}$ (C–O) values may be expected to provide reliable reference information for future laboratory investigations. Moreover, owing to the lower C–H bond dissociation energy, $CF_2ClC(O)OCH_3$ is more reactive toward hydrogen abstraction than $CF_3C(O)OCH_3$. This is reflected in the barrier height for hydrogen abstraction for $CF_2ClC(O)OCH_3$ and $CF_3C(O)OCH_3$. The barrier heights for hydrogen abstraction for $CF_2ClC(O)OCH_3$ as tabulated in Table 3 at both the MPWB1K and G2(MP2) levels are lower than the corresponding values for $CF_3C(O)OCH_3$ [35]. This result is in line with the fact that the replacement of one F atom in $CF_3C(O)OCH_3$ by Cl atom increases the reactivity of C–H bond toward hydrogen abstraction as reported by Blanco and Teruel [28].

The standard enthalpy of formation ($\Delta_fH°_{298}$) at 298 K for $CF_2ClC(O)OCH_3$ and the radical generated from hydrogen abstraction, $CF_2ClC(O)OCH_2$, can be valuable information for understanding the kinetics, mechanism and thermochemical properties of their reactions and most importantly for atmospheric modeling, but these values are not yet reported. The group-balanced isodesmic reactions, in which the number and types of bonds are conserved, are used as working chemical reactions herein to calculate the $\Delta_fH°_{298}$ for $CF_2ClC(O)OCH_3$ and $CF_2ClC(O)OCH_2$. Here, two isodesmic reactions [44] for each species are used to

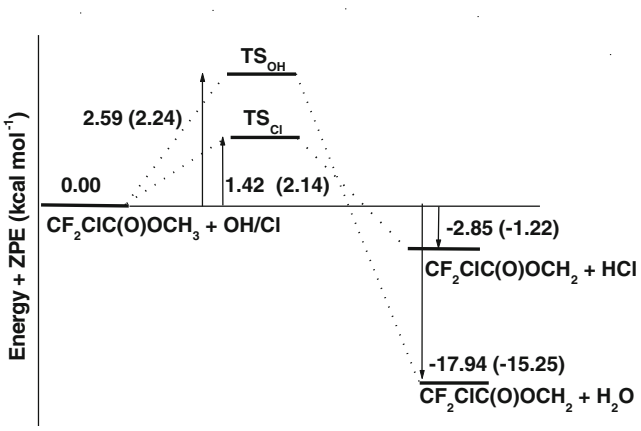


**Fig. 2** Potential energy diagram of the title reactions. The values in parentheses are ZPE corrected total energies at MPWB1K/6-31+G(d,p) level. Energy values are in kcal mol$^{-1}$

**Table 4** Calculated bond dissociation energy ($D^0_{298}$) (kcal mol$^{-1}$) for species at 298 K using G2(MP2)//MPWB1K/6-31+G(d,p) level

| Bond dissociation | G2(MP2)//MPWB1K/6-31+G(d,p) |
|---|---|
| C–H bond | |
| $CF_2ClC(O)OCH_3 \rightarrow CF_2ClC(O)OCH_2 + H$ | 102.13 |
| $CF_3C(O)OCH_3 \rightarrow CF_3C(O)OCH_2 + H$ | 110.32 |
| C–O bond | |
| $CF_2ClC(O)OCH_3 \rightarrow CF_2ClC(O) + CH_3O$ | 103.20 |
| $\rightarrow CF_2ClC(O)O + CH_3$ | 95.83 |
| $H_2O \rightarrow HO + H$ | 119.2 (119.0)[a] |
| $HCl \rightarrow H + Cl$ | 104.0 (103.1)[a] |

[a] Experimental values from Lide [43]

estimate the enthalpies of formation of the species. The used isodesmic reactions are as follows.

a. For $CF_2ClC(O)OCH_3$

$$CF_2ClC(O)OCH_3 + CH_4 + CH_3CH_3 + CH_3F \rightarrow CH_3COCH_3 + CH_3OCH_3 + CHF_3 + CH_3Cl \quad (R3)$$

$$CF_2ClC(O)OCH_3 + CH_3Cl \rightarrow CH_3C(O)OCH_3 + CF_2Cl_2 \quad (R4)$$

b. For $CF_2ClC(O)OCH_2$

$$CF_2ClC(O)OCH_2 + CH_4 \rightarrow CH_3C(O)OCH_3 + CF_2Cl \quad (R5)$$

$$CF_2ClC(O)OCH_2 + CH_4 \rightarrow CH_3 + CF_2ClC(O)OCH_3 \quad (R6)$$

We calculate the reaction enthalpies of R3–R6 and combine them with the known enthalpies of formation of the reference compounds involved in these reactions, $CH_4$: −17.89 kcal $mol^{-1}$ [45], $CHF_3$: −166.60 kcal $mol^{-1}$ [45], $CH_2F_2$: −107.71 kcal $mol^{-1}$ [45], $CH_3CH_3$: −20.04 kcal $mol^{-1}$ [46], $CH_3COCH_3$: −52.23 kcal $mol^{-1}$ [47], $CH_3OCH_3$: −43.9 kcal $mol^{-1}$ [48], $CH_3Cl$: −19.59 kcal $mol^{-1}$ [49], $CF_2Cl_2$: −117.72 kcal $mol^{-1}$ [50], $CF_2Cl$: −65.64 kcal $mol^{-1}$ [50], $CH_3C(O)OCH_3$: −98.0 kcal $mol^{-1}$ [51], $CH_3CONH_2$: −56.96 kcal $mol^{-1}$ [52] and $CH_3NH_2$: −5.52 kcal $mol^{-1}$ [53] and to evaluate the required enthalpies of formation. All of the geometrical parameters of the species in the isodesmic reactions are calculated at the MPWB1K/6-31+G(d,p) level and energies of the species are refined at the G2(MP2) level. The calculated values of enthalpies of formation are listed in Table 5 with available experimental data. Unfortunately, there are no experimental or theoretical reports on the $\Delta_fH°_{298}$ of the species $CF_2ClC(O)OCH_3$ and $CF_2ClC(O)OCH_2$ to make a comparison. In order to verify the accuracy of the above calculations, we have performed theoretical calculation on the $\Delta_fH°_{298}$ of $CH_3C(O)OCH_3$ and $CF_3C(O)OCH_3$ for which experimental $\Delta_fH°_{298}$ are reported. The following group-balanced isodesmic reactions are used.

$$CH_3C(O)OCH_3 + CH_3CH_3 \rightarrow CH_3COCH_3 + CH_3OCH_3 \quad (R7)$$

$$CH_3C(O)OCH_3 + CH_3NH_2 \rightarrow CH_3CONH_2 + CH_3OCH_3 \quad (R8)$$

$$CF_3C(O)OCH_3 + CH_4 \rightarrow CH_3C(O)OCH_3 + CHF_3 \quad (R9)$$

$$CF_3C(O)OCH_3 + CH_4 + CH_3CH_3 \rightarrow CH_3COCH_3 + CH_3OCH_3 + CHF_3 \quad (R10)$$

The calculated enthalpies of formation for $CH_3C(O)OCH_3$ and $CF_3C(O)OCH_3$ at G2(MP2)//MPWB1K/6-31+G(d,p) level using isodesmic reactions (R7–R10) are −98.60 and −243.35 kcal $mol^{-1}$, respectively. It is seen that our calculated $\Delta_fH°_{298}$ values for $CH_3C(O)OCH_3$ (−98.00 kcal $mol^{-1}$ [51]) and $CF_3C(O)OCH_3$ (−237.00 kcal $mol^{-1}$ [54]) is consistent with the literature values. The $\Delta_fH°_{298}$ value for $CF_2ClC(O)OCH_2$ radical can also be easily calculated from the reported $\Delta_rH°_{298}$ value for R1 in Table 1, the calculated $\Delta_fH°_{298}$ value for $CF_2ClC(O)OCH_3$ and the experimental $\Delta_fH°_{298}$ values for $H_2O$ (−57.8 kcal $mol^{-1}$) and OH (8.93 kcal $mol^{-1}$) radical [43]. The $\Delta_fH°_{298}$ for $CF_2ClC(O)OCH_2$ radical calculated from G2(MP2) results are −145.82 kcal $mol^{-1}$ which is very close to $\Delta_fH°_{298}$ value of −146.59 kcal $mol^{-1}$ calculated by using isodesmic reactions R(5) and R(6). This infers that the present theoretical calculations for $\Delta_fH°_{298}$ values for $CF_2ClC(O)OCH_3$ and $CF_2ClC(O)OCH_2$ species at G2(MP2) level may be reliable.

**Table 5** Enthalpies of formation ($_fH^0_{298}$) (kcal $mol^{-1}$) at 298 K from the isodesmic reactions

| Species | Isodesmic reaction schemes | G2(MP2) | Average value | Literature values |
|---|---|---|---|---|
| $CF_2ClC(O)OCH_3$ | R3 | −195.23 | −195.80 | – |
| | R4 | −196.38 | | |
| $CF_2ClC(O)OCH_2$ | R5 | −144.89 | −145.82 | – |
| | R6 | −146.75 | | |
| $CH_3C(O)OCH_3$ | R7 | −98.60 | −98.59 | −98.00[a] |
| | R8 | −98.58 | | |
| $CF_3C(O)OCH_3$ | R9 | −243.35 | −243.68 | −237.00[b] |
| | R10 | −244.01 | | |

[a] From [51]

[b] From [54]

## Rate constants

The rate constant for reactions (R1–R2) is calculated using canonical transition state theory (CTST) [55] that involves a semi-classical one-dimensional multiplicative tunneling correction factor given by the following expression:

$$k = \sigma\Gamma(T)\frac{k_BT}{h}\frac{Q^{\ddagger}_{TS}}{Q_R}\exp\frac{-\Delta E}{RT}, \quad (R11)$$

where, σ is the symmetry number, Γ(T) is the tunneling correction factor at temperature T. $Q^{\ddagger}_{TS}$ and $Q_R$ are the total partition functions for the transition states and reactants, respectively. ΔE, $k_B$ and h are the barrier height including ZPE, Boltzmann's and Planck's constants, respectively. The partition functions for the respective transition states and reactants at 298 K are obtained from the vibrational frequency calculation made at MPWB1K/6-31+G(d,p) level.

Barrier heights were estimated from the energy difference including ZPE between TSs and reactants. The partition functions for the respective transition states and reactants at 298 K are obtained from the vibrational frequencies calculation made at MPWB1K/6-31+G(d,p) level. The translational partition function was evaluated per unit volume. The total partition function was calculated as a product of the individual partition functions, the translational, rotational, vibrational, and electronic partition functions. Most of the vibrational modes were treated as quantum-mechanical separable harmonic oscillators except for lower vibration modes. The hindered-rotor approximation of Truhlar and Chuang [56] was used for calculating the partition function of lower vibration modes. During the calculation of total partition function for OH radical its electronic partition function was corrected by considering the excited state of OH radical with a 140 $cm^{-1}$ splitting by using the expression given below [57].

$$Q^{E}(OH) = 2 + 2\exp\left[-\frac{140(cm^{-1})hc_0}{K_B T}\right] \quad \text{(R12)}$$

Where, $C_0$, T and $K_B$ are velocity of light in vacuum, temperature and Boltzmann's constant, respectively. Similarly, the electronic partition function of Cl atom was corrected by considering the $^2P_{3/2}$ and $^2P_{1/2}$ electronic states with 881 $cm^{-1}$ splitting. The tunneling correction factor Γ(T) was calculated by using Wigner [58] and Eckart symmetrical barrier method [59–61]. Tunneling correction factor Γ(T) estimated by using Wigner and Eckart method are found be 3.32, 5.96 and 1.98, 2.48 for $TS_{OH}$ and $TS_{Cl}$, respectively. The calculated Γ(T) values by using Eckart symmetrical barrier are within the range of Johnston and Rapp estimated symmetrical tunneling barriers for chemical reactions [61]. The rate constant values for the reaction of $CF_2ClC(O)OCH_3$ + OH/Cl estimated by using Wigner's and Eckart tunneling correction along with the experimental values are presented in Table 6. The theoretically computed rate constant for H atom abstraction reaction of $CF_2ClC(O)OCH_3$ by OH radical as given by reaction (R1) by using Wigner and Eckart symmetrical method are found to be $0.51\times10^{-13}$ and $0.91\times10^{-13}$ $cm^3$ $molecule^{-1}$ $s^{-1}$, respectively at 298 K with available experimental value [$(1.0\pm0.2)\times10^{-13}$ $cm^3$ $molecule^{-1}$ $s^{-1}$] reported by Blanco and Teruel [28]. Whereas, the rate constant for H atom abstraction reaction of $CF_2ClC(O)OCH_3$ by Cl atom using Wigner and Eckart symmetrical method are found to be $0.96\times10^{-13}$ and $1.20\times10^{-13}$ $cm^3$ $molecule^{-1}$ $s^{-1}$, respectively at 298 K with reported experimental value of $(1.1\pm0.3)\times10^{-13}$ $cm^3$ $molecule^{-1}$ $s^{-1}$ [28]. Therefore, from our calculated rate constant it can be concluded that for the reaction of $CF_2ClC(O)OCH_3$ + OH, rate constant estimated by Eckart method is in very good agreement with the experimental one. However the rate constant calculated by Wigner's method slightly underestimated the experimental value. On the other hand for the reaction of $CF_2ClC(O)OCH_3$ + Cl our calculated rate constant using both Wigner's and Eckart method are in very good agreement with the available experimental value. In general, tropospheric lifetime ($\tau_{eff}$) of $CF_2ClC(O)OCH_3$ can be estimated by assuming that its removal from troposphere occurs only through the reactions with OH radical and Cl atom. Then ($\tau_{eff}$) can be expressed as [62],

**Table 6** Rate coefficients (units: $cm^3$ $molecule^{-1}$ $s^{-1}$) of H-abstraction from $-CH_3$ sites in $CF_2ClC(O)OCH_3$ at 298 K using G2(MP2) theory

| Species | $K_{Wigner}$ | $K_{Eckart\ Symmetrical}$ | $K_{Experimental}$ |
|---|---|---|---|
| $CF_2ClC(O)OCH_3$ + OH (R1) | $0.51\times10^{-13}$ | $0.91\times10^{-13}$ | $(1.0\pm0.2)\times10^{-13}$ |
| $CF_2ClC(O)OCH_3$ + Cl (R2) | $0.96\times10^{-13}$ | $1.20\times10^{-13}$ | $(1.1\pm0.3)\times10^{-13}$ |

$$1/(\tau_{\text{eff}}) = 1/(\tau_{\text{OH}}) + 1/(\tau_{\text{Cl}}) \quad \text{(R13)}$$

Where, $(\tau_{OH}) = (K_{OH}\times[OH])^{-1}$ and $(\tau_{Cl}) = (K_{Cl}\times[Cl])^{-1}$. Using the 298 K value of $K_{OH} = 0.91\times10^{-13}$ $cm^3$ $molecule^{-1}$ $s^{-1}$ and $K_{Cl} = 1.20\times10^{-13}$ $cm^3$ $molecule^{-1}$ $s^{-1}$, and the global average atmospheric OH and Cl concentrations of $8.8\times10^5$ and $1.0\times10^4$ molecule $cm^{-3}$ respectively [63, 64], the estimated atmospheric lifetime of $CF_2ClC(O)OCH_3$ is found to be around 142 days.

## Conclusions

The potential energy surface and reaction kinetics of the H abstraction reaction of $CF_2ClC(O)OCH_3$ + OH [Reaction (1)] and $CF_2ClC(O)OCH_3$ + Cl [Reaction (2)] are investigated at G2(MP2)//MPWB1K/6-31+G(d,p) level of theory. The barrier heights for these pathways are calculated to be 2.59 and 1.42 kcal $mol^{-1}$, respectively at G2(MP2) level. The calculated rate constants of the H abstraction reactions are consistent with the available experimental values. The $\Delta_f H°_{298}$ values for $CF_2ClC(O)OCH_3$, $CF_2ClC(O)OCH_2$ and $CF_3C(O)OCH_3$ are predicted to be −195.80, −145.82 and −243.68 kcal $mol^{-1}$, respectively. The estimated atmospheric life time of $CF_2ClC(O)OCH_3$ is expected to be around 142 days. The relatively short atmospheric life time of $CF_2ClC(O)OCH_3$ make their negligible contribution toward ozone depletion (ODP). These data can be useful for further thermo-kinetic modeling of other reactions involving these species.

**Acknowledgments** BKM is thankful to University Grants Commission, New Delhi for providing UGC-Dr. D. S. Kothari Post doctoral

Fellowship. Authors are also thankful to the reviewers for their constructive suggestions to improve the quality of the manuscripts.

## References


1. Molina MJ, Rowland FS (1974) Nature 249:810–814
2. Farman JD, Gardiner BG, Shanklin JD (1985) Nature 315:207–210
3. Tsai WT (2005) J Hazard Mater 119:69–78
4. Sekiya A, Misaki S (2000) J Fluorine Chem 101:215–221
5. Sherwood GJ (2000) US Patent No-6,148,634
6. Tucker MK (2012) Proceedings of The National Conference On Undergraduate Research (NCUR) Weber State University, Ogden P. No. 29–31
7. Ravishankara RA, Turnipseed AA, Jensen NR, Barone S, Mills M, Howark CJ, Solomon S (1994) Science 263:71–75
8. Hickson KM, Smith IWM (2001) Int J Chem Kinet 33:165–172
9. Urata S, Takada A, Uchimaru T, Chandra AK (2003) Chem Phys Lett 368:215–223
10. Singh HJ, Mishra BK (2010) J Mol Model 16:1473–1480
11. Singh HJ, Mishra BK (2011) J Mol Model 17:415–422
12. Chandra AK (2012) J Mol Model 18:4239–4247
13. Chen L, Kutsuna S, Tokuhashi K, Sekiya A (2004) Chem Phys Lett 400:563–568
14. Singh HJ, Mishra BK, Rao PK (2010) Bull Korean Chem Soc 31:3718–3722
15. Beach SD, Hickson KM, Smith IWM, Tuckett RP (2001) Phys Chem Chem Phys 3:3064–3069
16. Yang L, Liu JY, Wan SQ, Li ZS (2009) J Comput Chem 30:565–580
17. Blanco MB, Barnes I, Teruel MA (2010) J Phys Org Chem 23:950–954
18. Ninomiya Y, Kawasaki M, Guschin A, Molina LT, Molina MJ, Wallington TJ (2000) Environ Sci Technol 34:2973–2978
19. Dalmasso PR, Taccone RA, Nieto JD, Teruel MA, Lane SI (2006) Atmos Environ 40:7298–7303
20. Wingenter OW, Kubo MK, Blake NJ, Smith TW, Blake DR (1996) J Geophys Res 101:4331–4340
21. Sulback Andersen MP, Nielsen OJ, Wallington TJ, Hurley MD, DeMoore GW (2005) J Phys Chem A 109:3926–3934
22. Quan HD, Tamura M, Gao RX, Sekiya A (2003) J Fluorine Chem 120:131–134
23. Sekiya A, Quan HD, Tamura M, Gao RX, Murata J (2001) J Fluorine Chem 112:145–148
24. Chen QY, Duan JX (1993) Tetrahedron Lett 34:4241–4244
25. Su DB, Duan JX, Yu AJ, Chen QY (1993) J Fluorine Chem 65:11–14
26. Mcharek S, Sibille S, Nedelec JY, Perichon J (1991) J Organomettallic Chem 401:211–215
27. Mellouki A, Bras GL, Sidebottom H (2003) Chem Rev 103:5077–5096
28. Blanco MB, Teruel MA (2007) Chem Phys Lett 441:1–6
29. Blanco MB, Teruel MA (2007) Atmos Environ 41:7330–7338
30. Blanco MB, Bejan I, Barnes I, Wiesen P, Teruel MA (2008) Chem Phys Lett 453:18–23
31. Andersen VF, Berhanu TA, Nilsson EJK, Jørgensen S, Nielsen OJ, Wallington TJ, Johnson MS (2011) J Phys Chem A 115:8906–8919
32. Blanco MB, Bejan I, Barnes I, Wiesen P, Teruel M (2010) Environ Sci Technol 44:2354–2359
33. Frisch MJ et al. (2009) GAUSSIAN 09 (Revision B.01). Gaussian Inc, Wallingford
34. Zhao Y, Truhlar DG (2004) J Phys Chem A 108:6908–6918
35. Chakrabatty AK, Mishra BK, Bhattacharjee D, Deka RC (2012) Mol Phys. doi:10.1080/00268976.2012.747707
36. Mishra BK, Chakrabatty AK, Deka RC (2013) J Mol Model. doi:10.1007/s00894-013-1762-7
37. Gonzalez C, Schlegel HB (1989) J Chem Phys 90:2154–2161
38. Curtiss LA, Raghavachari K, Pople JA (1993) J Chem Phys 98:1293–1298
39. Kuchitsu K (1998) Structure of free polyatomic molecules basic data, 1. Springer, Berlin, p 58
40. Zhurko G, Zhurko D (2011) ChemCraft 1.6 Program Revision 1.6, Ivanovo, Russia
41. Hammond GS (1955) J Am Chem Soc 77:334–338
42. Troung NT, Truhlar DG (1990) J Chem Phys 93:1761–1769
43. Lide DR (ed) (2008–2009) CRC handbook of chemistry and physics, 89th edn. CRC, New York
44. Good DA, Fransisco JS (1998) J Phys Chem A 102:7143–7148
45. Chase MW Jr (1998) JANAF therochemical tables, 3rd edn. J Phys Chem Ref Data 9:1–1951
46. Pittam DA, Pilcher G (1972) J Chem Soc Faraday Trans 68:2224–2229
47. Wiberg KB, Crocker LS, Morgan KM (1991) J Am Chem Soc 113:3447–3450
48. Pilcher G, Pell AS, Coleman D (1964) J Trans Faraday Soc 60:499–505
49. Manion JA (2002) J Phys Chem Ref Data 31:123–172
50. Csontos J, Rolok Z, Das S, Kallay M (2010) J Phys Chem A 114:13093–13103
51. Hall HK Jr, Baldt JH (1971) J Am Chem Soc 93:140–145
52. Barnes DS, Pilcher G (1975) J Chem Thermodynamics 7:377–382
53. Wagman DD, Evans WH, Parker VB, Schumm RH, Halow I, Bailey SM, Churney KL, Nuttall RL (1982) J Phys Chem Ref Data 11:Suppl 2
54. Guthrie JP (1976) Can J Chem 54:202–209
55. Laidler KJ (2004) Chemical kinetics, 3rd edn. Pearson Education, New Delhi
56. Truhlar DG, Chuang YY (2000) J Chem Phys 112:1221–1228
57. Kaliginedi V, Ali MA, Rajakumar B (2012) Int J Quantum Chem 112:1066–1077
58. Wigner EP (1932) Z Phys Chem B19:203–216
59. Eckart C (1930) Phys Rev 35:1303–1309
60. Shavitt I (1959) J Chem Phys 31:1359–1367
61. Johnston HS, Rapp D (1961) J Am Chem Soc 83:1–9
62. Papadimitriou VC, Kambanis KG, Lazarou YG, Papagiannakopoulos P (2004) J Phys Chem A 108:2666–2674
63. Kurylo MJ, Orkin VL (2003) Chem Rev 103:5049–5076
64. Spicer CW, Chapman EG, Finlayson-Pitts BJ, Plastridge RA, Hubbe JM, Fast JD, Berkowitz CM (1998) Nature 394:353–356